The three body system δ Circini

Pavel Mayer, Petr Harmanec
Astronomical Institute of the Charles University, Faculty of Mathematics and Physics, V Holešovičkách 2, 180 00 Praha 8, Czech Republic

Hugues Sana
ESA / Space Telescope Science Institute, San Martin Drive, Baltimore, MD21218, USA
and

Jean-Baptiste Le Bouquin
UJF-Grenoble 1/CNRS-INSU, Institut de Planétologie et d'Astrophysique de Grenoble (IPAG) UMR 5274, Grenoble, France
mayer@cesnet.cz

ABSTRACT

Version August 12, 2014

Delta Cir is known as an O7.5 III eclipsing and spectroscopic binary with an eccentric orbit. Penny et al. discovered the presence of a third component in the *IUE* spectra. The eclipsing binary and the third body revolve around a common centre of gravity with a period of 1644 days in an eccentric orbit with the semimajor axis of 10 AU. We demonstrate the presence of the apsidal-line rotation with a period of $\approx$ 141 years, which is considerably longer than its theoretically predicted value, based on the published radii of the binary components derived from the Hipparchos $H_{\rm p}$ light curve. However, our new solution of the same light curve resulted in smaller radii and a better agreement between the observed and predicted period of the apsidal-line advance. There are indications that the third body is a binary. The object was resolved by VLTI with the PIONIER combiner; in June 2012 the separation was 3.78 mas, magnitude difference in the H region $1\overset{\rm m}{.}75$. This result means that (assuming the distance 770 pc) the inclination of the long orbit is $87\overset{\circ}{.}7$.

Subject headings: stars: early type — stars: binaries — stars: individual(δ Cir)

1. Introduction

There are not many known eclipsing binaries having such an early spectral type as δ Cir (HD 135240, HR 5664, HIP 74778). According to Walborn (1972), the integrated type is O7.5 III(f); but see later. The period is $3\overset{\rm d}{.}90$, brightness $V = 5\overset{\rm m}{.}05 - 5\overset{\rm m}{.}20$. The orbit is eccentric, so the rotation of the apside line is to be expected. Knowledge of the apse period is important, since there is only one other galactic binary of earlier spectral type with the known apsidal-line rotation period – HD 93205 (Morrell et al. 2001), and others of similar spectral types as δ Cir, V1007 Sco (Sana et al. 2001; Mayer et al. 2008), and HD 165052 (Ferrero et al. 2013).

The first three radial velocities (hereafter RVs) of δ Cir were obtained at the southern station of the Lick Observatory already in the year 1915

[1]Based on data products from observations made with ESO Telescopes at the La Silla Paranal Observatory under programs ID 65.N-0577, 67.B-0504, 074D-0300, 178.D-0361, 182.D-0356, 083.D-0589, 185.D-0056, 086.D-0997 and 087D-0946.

(Campbell 1928). Additional RVs were secured by Feast et al. (1957), Buscombe & Kennedy (1965), Buscombe & Kennedy (1969), and Conti et al. (1977). RVs and orbits for δ Cir were published by Thackeray & Emerson (1969, TE), Stickland et al. (1993, ST93), and Penny et al. (2001, Pe01). The results of these studies were similar; they all found a small eccentricity of the orbit (≈ 0.06) and semiamplitude $K_1 \approx 150$ km s^{-1}.

According to Pe01, the signature of a third body is present in the *IUE* spectra of δ Cir. Here we analyze the spectra from the ESO archive. The third body spectrum is present in these spectra, too. The mutual orbit of the eclipsing binary and the third body is clearly observed.

In the following, we describe the spectroscopic data we used (Sect. 2), how the RVs were measured and exploited for the orbital solutions (Sect. 3), discuss the probable elements of the third body (Sect. 4), disentangle the spectra (Sect. 5), analyze the interferometric data (Sect. 6), present the results of the light-curve solution (Sect. 7) and discuss the final results (Sect. 8).

2. The spectroscopic data

The spectra in the ESO archive consist of 2 UVES spectra from the years 2000–2001, 29 FEROS spectra from 2007–2009, and 95 HARPS spectra from 2009–2012[1]. We downloaded all HARPS and most of FEROS spectra as pipeline products. We also compiled all available RV measurements from the astronomical literature[2] and whenever necessary, calculated HJDs for them. Journal of all available RVs is in Table 1. Note that throughout this paper we use an abbreviation RJD = HJD−2400000.0 .

[1] UVES as well as FEROS and HARPS are echelle spectrographs. UVES is used with VLT at Paranal, FEROS (Kaufer & Pasquini 1998) with the 2.2-m ESO/MPI telescope at the ESO La Silla Observatory and provides spectra in the region from 3625 to 9125 Å with the resolving power of 48000. HARPS is a spectrograph connected with the 3.6-m ESO telescope, also at La Silla. Its spectral range is from 3781 to 6911 Å and the resolving power is 115000.

[2] Two remarks: (1) While inspecting local RV curves for the 3.9 d orbital period, we noted that two RVs derived by Buscombe & Kennedy (1965) on RJD 37043.2 and 37781.1 deviate very strongly from the RV curve. There is probably a date error: increasing both RJD for one day to 37044.2 and 37782.1 brings both RVs to agreement with the RV curve. (2) In the original paper, Feast et al. (1957) give a RV = −84 km s^{-1} for RJD 35252.4, while Thackeray & Emerson (1969) tabulate −88 km s^{-1} without any explanation. We adopted the original Feast's et al. value.

3. Analysis of radial velocities and orbital solutions

We first inspected the existing photographic RVs of the primary component. Several published photographic secondary velocities are probably rather uncertain. We also used the *IUE* RVs from Pe01. There are 41 *IUE* spectra taken over the course of 17 years. A large part, 29 of them, was obtained within ten days in September 1992. ST93 used only spectra from this short interval, and their solution of the primary RV curve has a rms = 2.3 km s^{-1}. Pe01 used all *IUE* spectra together with the Hα RVs (they obtained 18 CAT/CES spectra at the ESO La Silla Observatory and 3 spectra at the Mount Stromlo Observatory) and got rms = 8.2 km s^{-1}. They found a third component in the *IUE* spectra. We will show that the radial velocity of this third body varies; already the rms values cited above indicate that the position of the third line must vary, naturally due to the third-body motion around a common centre of gravity with the 3.9 d binary. Such an explanation of the unexpectedly large rms has already been put forward by TE. ST93 also noted that their systemic velocity differs from that derived by TE and explained the difference by the presence of a third body. Pe01 got different systemic velocities for the IUE and Hα spectra. For the primary RVs, the difference amounted to 19.6 km s^{-1}. Pe01 suggested that this difference might be due to the fact that the corresponding lines were formed in different layers in an expanding stellar atmosphere. However, we note that their Hα and IUE spectra were obtained in different times, so in view of the results from the ESO spectra, the true reason of the difference might well be the orbital motion in the three-body system. In the Pe01 solution, the difference, 19.6 km s^{-1}, was added to the Hα velocities, so we subtracted this value to use the originally measured RVs.

The ESO FEROS and HARPS spectra were always taken during rather short time intervals, every year from 2007 to 2012. The contribution of the third body to the line spectrum is obviously present in the ESO spectra, too; it is needed to fill

Table 1

Journal of available RVs of δ Cir

Spg.No.	RJD range	No. of RVs	Observatory/instrument	Source
1	20682.65-20740.49	3/0	Lick 1-prism	Campbell (1928)
2	34522.37-35284.38	3/0	Radcliffe	Feast et al. (1957)
3	36014.00-37781.10	3/0	MtStromlo	Buscombe & Kennedy (1965)
4	38243.93-38628.87	4/0	MtStromlo coude	Buscombe & Kennedy (1969)
2	39363.20-39906.62	24/5	Radcliffe	Thackeray & Emerson (1969)
3	39703.87-39704.86	2/0	MtStromlo	Buscombe & Kennedy (1969)
5	42115.81	1/0	Cerro Tollolo	Conti et al. (1977)
6	43756.92-49964.99	41/41	IUE	Penny et al. (2001)
7	49867.54-49874.79	18/14	ESO coude feed	Penny et al. (2001)
8	50152.14-50155.08	3/3	MtStromlo CCD	Penny et al. (2001)
9	51653.86-52012.88	2/2	ESO UVES	This paper
10	54277.54-55698.72	29/16	ESO FEROS	This paper
11	55003.44-56136.47	95/50	ESO HARPS	This paper

Table 2
FEROS and HARPS Radial Velocities of δ Cir

RJD	Phase[a]	Primary RV	Secondary RV	Tertiary RV
54277.5318	0.915	36.6		
54278.5352	0.172	181.4	−261	−45
54279.5359	0.428	−22.2		
54280.4936	0.674	−130.9	288	−59
54281.4853	0.928	47.5		
54282.4858	0.184	180.3	−238	−38
54283.5279	0.451	−43.1		
54284.4521	0.688	−125.5	274	−23
54285.5075	0.958	82.0		−49
54286.5188	0.218	156.9	−213	−35
54298.4766	0.282	109.1		−69
54299.4835	0.540	−102.3	239	−38
54300.4733	0.793	−83.2		
54300.4752	0.794	−82.2		−34
54301.4741	0.050	162.7	−230	−53
54302.4761	0.306	86.0		
54660.4685	0.042	136.5	−249	−34
54660.4707	0.042	135.0	−250	−31
54662.6006	0.588	−139.5	258	26
54663.5865	0.841	−66.0		−5
54664.5370	0.084	161.3	−268	−19
54665.5846	0.353	35.3		
54666.4724	0.580	−137.0	240	24
54667.4764	0.838	−68.3		−4
54667.5368	0.823	−51.1		−5
54953.7739	0.201	136.1	−264	−14
55003.4383	0.927	15.8		
55003.4419	0.928	16.9		
55004.4810	0.194	129.1	−268	
55004.4871	0.196	129.0	−269	
55005.7396	0.517	−116.0	201	
55006.4428	0.697	−158.0	265	
55006.4463	0.698	−157.4	265	
55007.4539	0.956	45.6		
55008.4769	0.218	119.9	−259	
55009.5571	0.493	−103.2	159	
55010.4657	0.728	−148.6	249	
55011.6215	0.024	105.9	−244	
55012.4466	0.236	111.1	−244	
55028.4563	0.338	34.7		
55028.4584	0.339	34.3		

TABLE 2—*Continued*

RJD	Phase[a]	Primary RV	Secondary RV	Tertiary RV
55029.4521	0.593	−147.6	240	70
55029.4547	0.594	−147.5	239	70
55029.4568	0.594	−147.9	240	70
55029.5183	0.610	−153.4	245	60
55029.5204	0.611	−153.1	245	77
55029.5912	0.629	−155.3	245	78
55029.6397	0.641	−153.9	248	72
55029.7290	0.664	−155.4		
55030.7379	0.923	17.6		
55030.7400	0.923	17.5		
55030.7428	0.924	19.0		
55031.4752	0.112	150.4	−305	−9
55360.5292	0.432	−56.6		21
55360.5325	0.432	−58.9		
55360.5377	0.434	−58.2		
55361.5137	0.684	−162.3	231	52
55364.4813	0.444	−70.6		
55365.4783	0.700	−155.5	224	27
55365.4825	0.701	−157.6	226	34
55368.4988	0.474	−94.9		50
55369.4953	0.729	−147.7	210	52
55379.4614	0.283	71.1		12
55380.4548	0.537	−134.5	191	44
55382.6112	0.090	145.1	−304	22
55383.7235	0.375	−8.6		
55736.5051	0.775	−79.7		
55736.5089	0.776	−80.4		
55737.5312	0.038	163.9	−206	−43
55737.5371	0.039	164.0	−206	−46
55738.5368	0.296	107.4		−21
55738.5425	0.297	105.5		−28
55739.5341	0.551	−94.3	258	−40
55739.5389	0.552	−95.8	258	−35
55740.5316	0.807	−56.1	203	
55740.5390	0.809	−53.7	204	
55741.5105	0.058	176.2	−254	−59
55741.5162	0.059	177.2	−255	−52
55742.4591	0.301	100.5		
55742.4746	0.305	98.3		
55743.6485	0.605	−117.9	294	−48
55744.5190	0.828	−35.8		

the observed He I line profiles. In this study, the FEROS as well as HARPS spectra were smoothed to the resolution 0.06 Å and rectified using the program SPEFO (Horn et al. 1996, Škoda 1996). We also measured their RVs using a fit with three Gaussians, and – in the second step – we applied spectral disentangling (Sect. 5).

In the He II lines 4541 and 5411 Å no traces of the secondary lines are present. Also no contribution from the third body should be there since this object is – according to Pe01 – cooler than the secondary. Therefore, we measured the primary RVs in these lines (in He II 4686 Å there is a weak contribution of the secondary). The secondary RVs were measured in the line He I 5876 Å, because the separation of the secondary from the primary lines at quadratures is the best here. The secondary velocities were measured only in cases where their separation enabled a reliable Gaussian fit, i.e. close to quadratures.

The resulting RVs are listed in Table 3. In the first 13 HARPS spectra, a strong fringing was identified by Poretti et al. (2013). However, we succeeded to find the period and amplitude of the fringes and to remove them from the spectra.

We derived various orbital solutions from the measured RVs using the program `FOTEL` (Hadrava 2004a). When a joint solution for all primary RVs from the ESO spectra of δ Cir was derived, the result was quite disappointing: large deviations were present, with rms 21 km s^{-1}. But when we splitted the available RVs into subsets covering short time intervals and assigned individual systemic velocity $V\gamma$ to each of them (which is easy to do with `FOTEL`), a solution with a much lower rms was obtained. For instance, quite different $V\gamma$ velocities were obtained for the FEROS spectra from 2007 and from 2008, and for the HARPS spectra from 2010 and 2011.

We therefore selected only series of spectra, which cover short time intervals and derived individual $V\gamma$ velocities for them. Our selection and the results are listed in Table 3 and shown in Fig. 1. The motion in the mutual orbit is clearly visible. Its period depends mostly on the ESO data, and it must be close to 4.5 years, with semi-amplitude ≈ 24 km s^{-1}. These values fit the older data too, and both orbits, with the periods of 3.9 d as well as 4.5 year, can be solved. But there is also another way how to use the RVs. The program `FOTEL` allows to solve both orbits in a hierarchic system simultaneously, with the advantage that all RVs, not only those in the time-limited groups, can be used. The solution which includes all old and new RVs is shown in Table 4. The RVs were weighted by weights inversely proportial to the squares of rms errors of individual datasets.

There is certainly a measurable increase of the longitude of the periastron over the time interval from the *IUE* spectra to the ESO spectra. However, the value obtained by TE disagrees with the trend defined by other sources. This could, of course, be related to the limited number of photographic RVs available to TE and the effects of the motion in the wide orbit.

To verify this suspicion, we split the RVs into two data sets, before RJD 43000 and more recent ones, and derived separate solutions for them modelling both orbits simultaneously. We obtained periastron argument values of $\omega = 133° \pm 25\circ$ for the epoch RJD 31996 and $\omega = 299\overset{\circ}{.}9 \pm 6\overset{\circ}{.}4$ for the epoch RJD 54286. This would imply the rate of apsidal advance $\dot{\omega} = 0\overset{\circ}{.}0075$ per day.

We show the measured RVs in Fig. 2. Due to the apside-line advance only RVs from a limited time interval – the RVs measured from HARPS spectra – are shown. The RVs are corrected by the systemic velocity determined for individual seasons (Table 3). All differences of observed and expected velocities in the third-body system are plotted in Fig. 3.

4. The third body and its mutual orbit with the eclipsing binary

A relative contribution of the primary is the least pronounced in the He I line 4922 Å. This gives the best chance to measure the line of the tertiary here, similarly as in the case of the secondary, i.e. near quadratures. The He I 4026 Å line, although strongest among the He I lines, is not suitable for the Gaussian fitting. For the primary component, this line is blended with the He II 4025 Å line and this would lead to an incorrectly measured RV of the tertiary. The He I 4026 Å line is suitable for disentangling, however, for which the line blending does not represent any problem.

The systemic velocities of the eclipsing binary (ESO data only), together with the measured RVs of the third line, are displayed in Fig. 4. Clearly,

TABLE 2—*Continued*

RJD	Phase[a]	Primary RV	Secondary RV	Tertiary RV
55744.5257	0.830	−34.4		
55745.4633	0.070	182.7	−260	−60
55745.4700	0.072	184.3	−251	
55760.4660	0.915	45.3		
55760.4705	0.916	50.0		
55760.4901	0.921	57.8		
55762.4632	0.427	−10.8		
56103.4443	0.803	−77.5		
56103.4500	0.804	−78.4		
56104.4482	0.060	156.8	−257	−50
56104.4521	0.061	157.3	−262	−50
56105.4502	0.317	73.4		
56105.4544	0.318	72.9		
56106.4533	0.574	−117.3		
56106.4574	0.575	−121.3		
56106.4631	0.576	−119.7	246	−28
56106.4720	0.578	−120.5	246	−22
56108.4500	0.085	167.6	−277	−24
56108.4582	0.087	166.5	−278	−32
56109.4479	0.341	56.7		
56109.4525	0.342	56.7		
56109.4575	0.344	55.5		
56110.4490	0.598	−130.2	265	−14
56110.4563	0.600	−129.3	278	−16
56111.4608	0.857	−29.1		
56111.4675	0.859	−25.8		
56113.4493	0.366	32.5		
56113.4562	0.368	29.9		
56132.4625	0.238	134.4	−224	−42
56133.4607	0.494	−76.9		
56133.4639	0.495	−78.4		
56133.4682	0.496	−80.8		
56134.4657	0.752	−114.7	233	−26
56134.4736	0.754	−112.2	233	−10
56135.4592	0.006	114.3	−193	−24
56135.4660	0.008	113.9	−194	−24
56136.4590	0.263	117.4	−195	
56136.4682	0.172	112.8	−193	

[a]Orbital phases are calculated for the final ephemeris of Table 3 of the $3\overset{d}{.}9$ orbit: HJD $2454285.66 + 3\overset{d}{.}902463 \times E$.

Table 3

Seasons with δ Cir Spectral Observations

RJD range	Center of the Interval	Number of measurements	$V\gamma$ km s^{-1}	rms km s^{-1}	ω deg	Source of Data
39594 to 39723	1967.7	19	9.2	12.3	296 ± 17	TE[a]
44449 to 44460	1980.2	6	17.5	9.9	229 ± 10	Pe01, *IUE* RVs[b]
48885 to 48894	1992.8	29	−8.3	4.9	257 ± 3	Pe01, *IUE* RVs[c]
49867 to 49874	1995.4	21	−0.7	9.5	272 ± 3	Pe01, Hα
50152 to 50155	1996.2	3	−16.5	8.8		Pe01, Hα
54277 to 54302	2007.6	16	18.6	4.6	323 ± 4	FEROS 2007
54660 to 54667	2008.7	9	−0.8	4.9	305 ± 4	FEROS 2008
55028 to 55031	2009.6	14	−7.9	3.5	316 ± 4	HARPS 2009
55360 to 55383	2010.5	13	−14.7	2.4	310 ± 4	HARPS 2010
55736 to 55762	2011.6	23	29.5	3.2	317 ± 3	HARPS 2011
56103 to 56113	2012.5	21	13.6	2.7	312 ± 3	HARPS 2012/1
56132 to 56136	2012.6	10	9.5	2.2	309 ± 3	HARPS 2012/2

[a]Only data from the year 1967.

[b]Data from the years 1979 and 1980.

[c]Only data from September 1992.

Table 4

The Orbit of the Eclipsing Binary and the Mutual Orbit with the Third Body based on the Gaussian-fit RVs and a FOTEL Triple-star Solution

Element	3.9 d Orbit	1644 d Orbit
Sidereal period P [days]	3.902463(6)	1644(3)
Epoch of periastron [RJD]	54285.66(5)	37482(27)
Eccentricity e	0.0601(48)	0.415(32)
Longitude of periastron ω [deg]	308.3(4.7)	106(6)
Semiamplitudes K_1 and K_3 [km s^{-1}]	153.9(1.5)	23.6
Semiamplitude K_2 [km s^{-1}]	284.17	
Systemic velocity $V\gamma$ [km s^{-1}]	3.5	3.1
Apsidal advance $\dot{\omega}$ [deg/day]	0.00696(15)	
Mass ratio m_2/m_1	0.546(3)	
$m_1 \sin i^3$ [M$_\odot$]	22.21	
$m_2 \sin i^3$ [M$_\odot$]	12.13	
$a \sin i$ [R$_\odot$]	33.90	

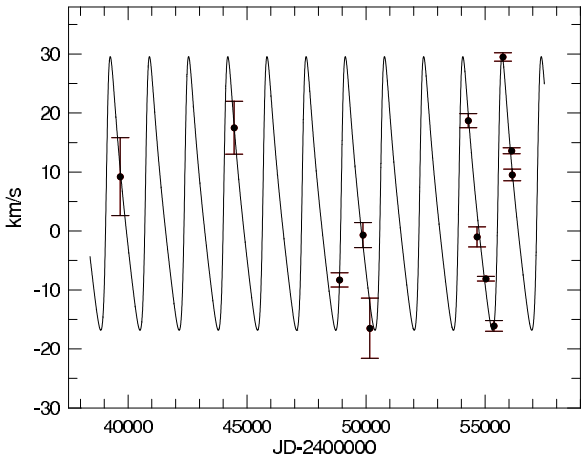

Fig. 1.— Possible solution of the third body orbit in δ Cir: period 4.5 years, semiamplitude 23.6 km s^{-1}.

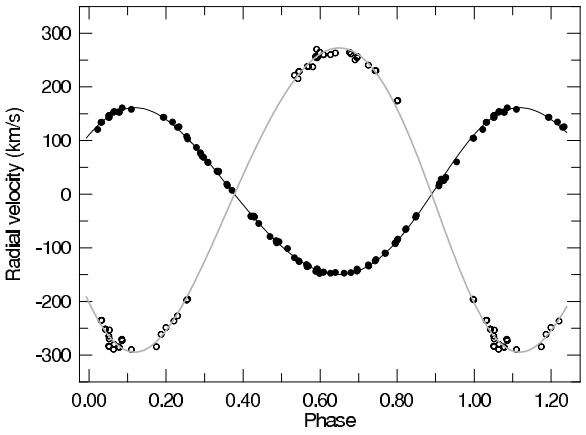

Fig. 2.— The RVs measured in HARPS spectra corrected to a common systemic velocity. Full circles – primary RVs, open circles – secondary RVs.

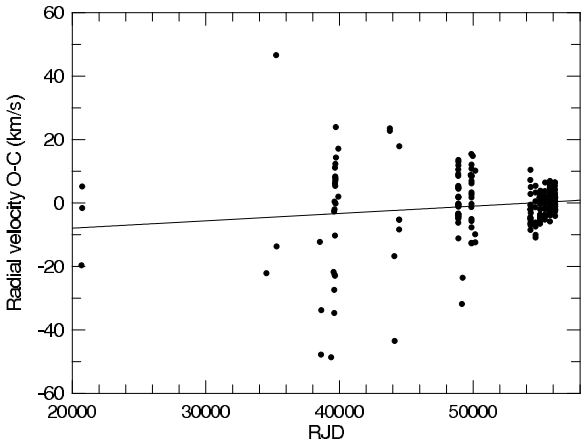

Fig. 3.— Differences of observed and expected velocities in the third-body system.

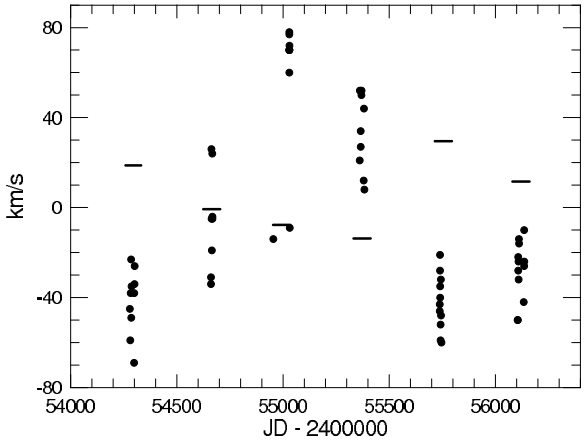

Fig. 4.— Systemic velocities of the eclipsing binary (short horizontal lines) and measured RVs of the third line (full circles) according to the FEROS and HARPS spectra.

the third line velocity varies in *antiphase* with the systemic velocity, confirming the mutual orbital motion of both objects. The amplitude of the RV of the third line appears to be about 2.3 times larger than the amplitude of the orbital motion of the 3.9 d binary in the long orbit as derived from its varying systemic velocity. Using the program KOREL (Hadrava 2004b), it was possible to estimate the semiamplitude of the third-body orbit K_3 more accurately (see sect. 5 and Table 5).

The third body RVs shown in Fig. 4 were obtained when only a single line was considered to represent the third body. But it appears that in some cases a two-line representation of the third light is necessary. In Fig. 5 an example of such profile is given. It is usually difficult, however, to decide which option is better as the fit qualities of both – three or four Gaussians – are quite comparable. Nevertheless, a possibility that the third body is a binary exists. Besides the cases where a two-line representation is clearly better, that possibility is also indicated by the large scatter of all measurements of the third line RVs. In spite of all effort, we have not succeeded to find the period of the putative second binary. However, from the cases where a four-Gaussian fit appears superiour, we suspect that the period should be of the order of several days.

5. Disentangling of spectra

Although the RVs measured using Gaussians gave acceptable results, more reliable elements can be obtained via spectral disentangling. We used the program KOREL (Hadrava 2004b; details about the application see Mayer et al. 2013) and applied it to three different spectral segments, containing the lines He I 4026, He I 4922, and He II 5411 Å. In the case of the He II 5411 Å line, no traces of the secondary or tertiary components were detected, so only the line of the primary was disentangled. Since the RVs which were used by the program FOTEL cover longer time interval we assumed the values of both orbital periods derived by this program (Table 4) when applying KOREL.

We first investigated the dependence of the sum of squares of residuals on various elements, namely the semiamplitudes and mass ratios of both recognized subsystems, keeping the orbital periods and the value of the apsidal advance of the 3.9 d orbit fixed at values obtained from the FOTEL triple-star solution. After finding the values of the semiamplitudes and mass ratios corresponding to the lowest sum of residuals in each studied region, we used them as starting values and run a number of solutions for all elements (but the periods and the apsidal advance), kicking the initial values to different directions. The solutions with the lowest sum of residuals are summarized in Table 5 and the corresponding disentangled line profiles are in Fig. 6.

The values of the mass ratios could not, of course, be derived for the He II 5411 Å region. The equivalent widths (EWs) of several lines as measured on the disentangled spectra are listed in Table 6.

As KOREL does not provide an estimate of the errors of the elements, Table 5 contains also the mean values of all three solutions and their rms errors. While there is a satisfactory agreement of the values of the majority of orbital elements among the three solutions, there is a striking difference in the value of the mass ratio of the outer orbit between the solution based on the He I 4026 Å and on He I 4922 Å lines. In our opinion, this might indicate that the third body is indeed a binary and that the line blending between the components of this pair of stars is different for the two investigated lines. This implies that before the resolution of this pair of stars, the mass ratio of the 1644 d system must be considered uncertain.

The plots of disentangled line profiles show that the secondary He I 4922 Å line is asymmetric due to the blend with the O II line 4925 Å. But the tertiary line is symmetric (although originating in a component/components of similar temperature) and of different shape. As a matter of fact, its shape is a perfect sinusoid. Such a profile would result as an integration of the orbital motion in the putative second binary system. Therefore, it supports our suspicion that the third body is indeed another binary. Guided by the opinion reached when these lines were measured using Gaussians, the EW ratio of the putative second binary lines might be about 2/3, with similar mass ratio; so the theoretical curve has been calculated as a sum of two sinusoids. Apparently, also the contribution of the "secondary" represents the wings of the profile well.

Table 5
KOREL Solutions

Element	Line 4923 Å	Line 4026 Å	Line 5411 Å	Mean
3.9 d Orbit				
$T_{\rm periastr.}[RJD]$	54285.612	54285.634	54285.672	54285.639
e	0.066	0.072	0.067	0.068
ω [deg]	304.6	307.0	309.6	307.1
K_1 [km s^{-1}]	157.4	156.3	156.6	156.8
K_1/K_2	0.558	0.560	–	0.559
K_2 [km s^{-1}]	282.1	279.1	–	280.4
$a \sin i$ [R$_\odot$]	33.84	33.51	–	33.65
1644 d Orbit				
$T_{\rm periastr.}$ [RJD]	37469.4	37485.0	37497.5	37484.0
e	0.440	0.468	0.339	0.416
ω [deg]	284.9	286.7	280.5	284.0
K_{1+2} [km s^{-1}]	22.2	23.0	22.0	22.4
K_{1+2}/K_3	0.362	0.452	–	0.407
K_3 [km s^{-1}]	61.3	50.9	–	55.0
$a \sin i$ [AU]	11.33	9.87	–	10.64

Table 6
Equivalent Widths

Measurements:	Primary	Secondary	Tertiary
EW 4922 Å	0.183	0.084	0.061
EW 4686 Å	0.44	0.05	0.000
Theory:			
$T_{\rm eff}$ assumed	34000	29000	28000
$\log g$ assumed	3.75	4.1	4.2
$L_{\rm i}$	0.66	0.16	0.13
EW 4922 Å	0.25	0.64	0.68
EW 4922/$L_{\rm i}$	0.28	0.52	0.47

6. Interferometry

Independently of the spectroscopic detection, the third body was discovered by interferometry. δ Cir was observed in June 2012 (RJD 56090.554) with VLTI and the PIONIER combiner (Le Bouquin et al. 2011); the separation was 3.87 mas and magnitude difference $1\overset{\mathrm{m}}{.}75$ in the H band.

The observed separation ρ can be calculated as

$$\rho^2 \quad = \quad \left(\frac{a(1-e^2)}{(1+e.\cos\nu)}\right)^2 (1-\sin^2(\omega+\nu).\sin^2 i).$$

With the elements of the 1644 d orbit (Table 5), the true anomaly ν equals 150° for the given date, and the inclination can be calculated as $i = 87\overset{\circ}{.}7$. A large inclination is needed to satisfy the solution of the long orbit as it will be discussed in the next section.

7. Light-curve solution, physical elements of the system, and the apsidal advance

The light variability of δ Cir was first reported by Cousins & Stoy (1962). However, the only published light curve (lc) of δ Cir is based on the *Hipparcos* $H_{\rm p}$ photometry (Perryman & ESA 1997). We noted that Thackeray & Emerson (1969) mentioned receiving unpublished Cape V photometry of δ Cir from Dr Cousins, indicative of binary eclipses. At our request, Dr David Kilkenny very kindly searched in the archival materials remaining after the late Drs Cousins and Thackeray. Regrettably, he was unable to find the original photometric observations but he did find a plot of the V magnitude vs. phase in the folder with the correspondence of Dr Thackeray. To preserve this previous piece of information, we reproduce the original plot in Fig. 7. Assuming Thackeray & Emerson (1969) ephemeris, we were able to reconstruct the light curve and use it also along with the *Hipparcos* H_p photometry. In doing so, we took into account the remark of Thackeray & Emerson (1969) that the Cousin's photometry covers an interval of 5000 days. We therefore assumed that the mean epoch of the photometry falls into the year 1960 and created artificially fictitious Julian dates corresponding to the phases of observations for RJDs 37000-37004.

A solution of the *Hipparcos* lc was derived by Pe01, but they used a program designed for circular orbits only. It can be seen in Fig. 4 of Pe01 that the observed widths of the 3.9 d binary eclipses are *narrower* than the calculated lc and the observed maxima are flatter. It was therefore deemed useful to obtain another light-curve solution, based on a modern program. We used the program `PHOEBE` (Prša & Zwitter 2005). The projected semimajor axis $a\sin i$ and the binary mass ratio following from the mean `KOREL` solution were fixed in `PHOEBE`. Since all components of δ Cir are hot stars we fixed both the albedos and the gravity darkering coefficients equal to 1. The square-root limb darkening coefficients were used. The value of the sidereal orbital period was kept fixed from the final `FOTEL` solution of Table 4. After a few trials we found that the scarsely covered eclipses cannot guarantee a unique solution; the space of possible solutions with nearly identical quality of the fit was immense. To circumwent this unpleasant situation, we simply assumed the temperatures and relative photometric radii corrsponding to the known spectral classification of the eclipsing components, and also the light contibution of the third body as found from the interferometry and fixed them in the light curve solution. The only free parameters of the solution were the epoch, longitude of the periastron passage, orbital inclination, and the relative luminosity of the primary. Keeping even the inclination of the orbit fixed from this solution, we then derived an independent solution also for the reconstructed V light curve from Cousin's observations. The results are summarized in Table 8 and the theoretical and observed light curves are compared in Fig. 8.

One can see that the fit is very good and in this sense it confirms that the light curves do not contradict the temperatures and radii we adopted. More notably, the values of the longitude of the periastron basically confirm the rate of apsidal advance deduced from spectroscopy. It is clear, however, that a really accurate determination of the rate of apsidal advance will require a new, accurate light curve (and/or continuing spectroscopic observations). At present, no good photometry regrettably exists. The ASAS data (Pojmanski 2002) are quite noisy (as it is common for such bright stars), and only a rough time of a normal minimum can be deduced: RJD 54601.383 (according to our ephemeris, a secondary minimum should appear at RJD 54601.381). Any shift of the phase of the secondary minimum from 0.5 (as

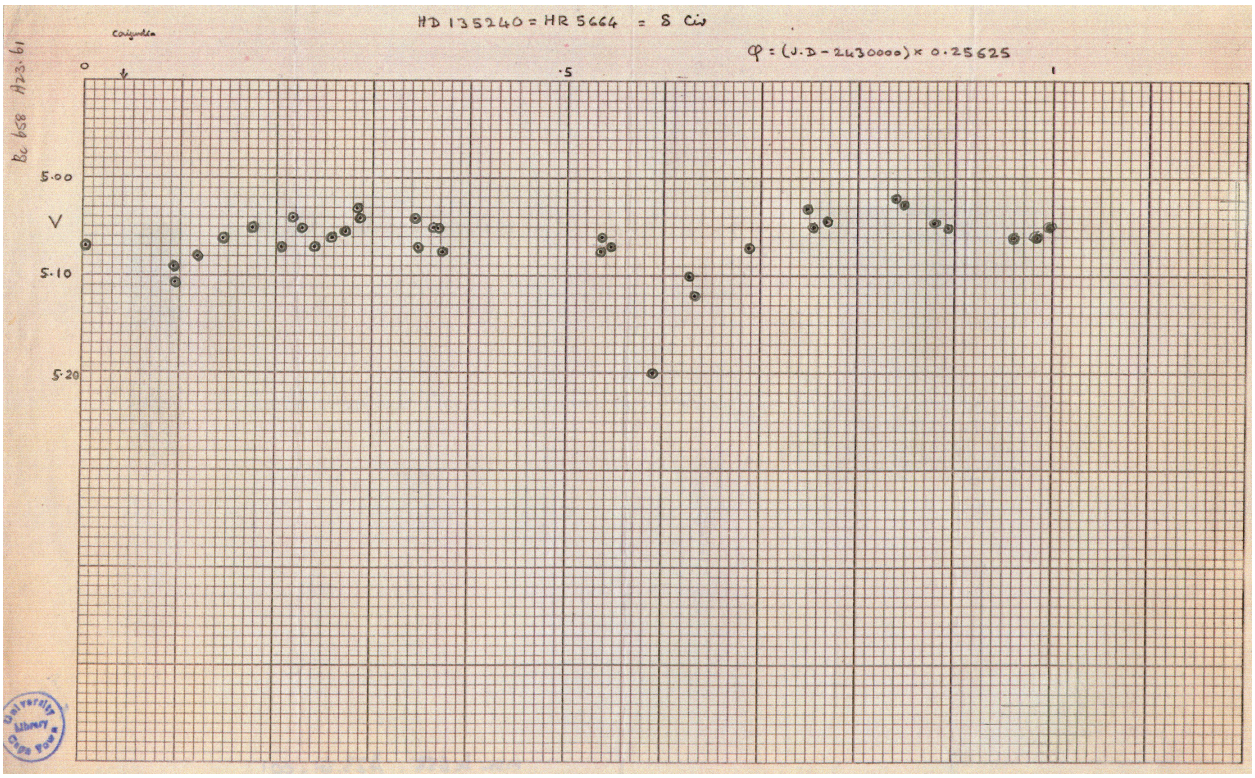

Fig. 7.— A reproduction of the original phase diagram based on Dr Cousins' V photometry found in the correspondence of Dr Thackeray by Dr Kilkenny.

it is observed in the *Hipparcos* photometry) is uncertain.

8. Discussion and conclusions

From the elements of the mutual orbit as presented in Table 4, the minimum mass of the eclipsing binary is 43.6 $M_\odot$ and the mass of the third body 18.7 $M_\odot$. However, the total mass of the eclipsing binary (see sect. 5) is only 36 $M_\odot$. Therefore, K_3 is very probably smaller than 55 km s^{-1}; e.g. with 51 km s^{-1} the minimum mass of the eclipsing binary is 36 $M_\odot$. Certainly the inclination has to be large, which would be in agreement with the interferometry.

The mass of the third body, as it follows from the solution of the long orbit, is large (larger than the mass of the secondary) even with the assumed $K_3 = 51$ km s^{-1}. It would agree better with the interferometric magnitude difference as well as with the spectroscopic evidence if this body is a binary.

We calculated the expected apside-line period using the evolutionary models by Claret (2004). The theoretical period depends strongly on the radii, and with the radii derived by Pe01 ($R_{\rm pri} = 10.2$ and $R_{\rm sec} = 6.4$ $R_\odot$; polar radii), the apsidal period should be ≈ 62 years (including the general relativity contribution, which is $0\overset{\circ}{.}00247$ per cycle). In order to reproduce the observed apsidal period, the radii would have to be smaller. With our radii (Table 7), the corresponding theoretical apside-rotation period is 85 yrs, closer to but still shorter than the observed one.

The apside-line period can, of course, be affected by the third body. From theoretical considerations it is clear that the effect increases if the ratio of semimajor axis $a_{\rm long}/a_{\rm short}$ is becoming smaller, and if the mutual inclination increases. In the case of δ Cir the ratio of axes is 66, the inclination $11\overset{\circ}{.}8 < i < 16\overset{\circ}{.}4$ (since $i_{\rm long} = 87\overset{\circ}{.}7$ and $i_{\rm short} = 75\overset{\circ}{.}9$), also e_1 is small. Then the formula by Söderhjelm (1984, eq. 25) might give an approximate idea about the magnitude of the effect (although it is valid for $e = 0$, and $i = 0$ only). According to it, the apsidal period – due to the third body only – would be ≈ 1500 yrs. As the expected period is ≈ 100 yrs, the effect migh be only of the order of several percents, which is smaller than the present errors of theoretical estimates as well as of observational value.

Once more we repeat that a new, accurate and complete multicolor light curve is highly desirable and crucial for a reliable determination of the basic properties of the binary.

We also note that our new radius of the primary is not consistent with the radius expected for the O7.5 III classification, for which e.g. Martins et al. (2005) give $R \approx 14$ $R_\odot$. Another classification was published by a team from the Yerkes Observatory (Hiltner et al. 1969): O8.5 V. Pe01 classified the primary component using IUE spectra as O7 III-V. We measured the 4471/4541 ratio as $\log W' = +0.21$ (Conti & Alschuler 1971), the corresponding type is O 8. Therefore we suspect that the individual classification of the primary is O8 IV; such luminosity class is supported also by the He I 4143 Å line when compared to a synthetic spectrum. Pe01 claimed that the primary mass of δ Cir is smaller than would correspond to the given spectral type. We got larger semiamplitudes of RVs, so now the mass is fully consistent with the value by Martins et al. (2005).

There are several early B type stars closer than 10 arcmin to δ Cir (HD 135160, 135241, 135332), however their distances are not well known and it is not possible to suggest that δ Cir is a member of a group.

In spite of some uncertainties in the solutions of the RV and light curves, an acceptable model of the system of δ Cir is obtained. Further interferometric data are needed to see if the separation and change of the position angle follow the prediction.

Our very sincere thanks are due to Dr David Kilkenny, who very kindly searched on several places in the archives to locate Dr Cousins photometry of δ Cir and provided us with a phase plot of V observations, which he found. PM and PH were supported by the grant P209/10/0715 of the Czech Science Foundation and also from the research program MSM0021620860. We profitted from the use of the electronic NASA/ADS bibliographical service and the Strasbourg CDS SIMBAD database.

REFERENCES

Buscombe, W., & Kennedy, P.M. 1965, MNRAS, 130, 281

Table 7

PHOEBE Light Curve Solution and Physical Elements of δ Cir

Element	Primary	System	Secondary
Inclination [deg]		75.81 ± 0.10	
Semimajor Axis [$R_\odot$]		34.7	
Relative Radii[a]	0.265		0.165
$T_{\rm eff}$ [K]	34000[a]		29000[a]
Masses [$M_\odot$]	23.6		13.2
Radii [$R_\odot$]	9.20		5.73
$M_{\rm bol}$ [mag]	-7.76		-6.05
$\log g$ [cgs]	3.88		4.04
$L_{\rm V}$[b] (Cape)	0.6460 ± 0.0020		0.1877
$L_{\rm Hp}$[b] (Hip)	0.6485 ± 0.0005		0.1852
L_3		0.1663[a]	
$T_{\rm min.I}$ (Cape) [RJD]		37003.320 ± 0.011	
ω (Cape) [deg]		185 ± 38	
$T_{\rm min.I}$ (Hip) [RJD]		48398.1212 ± 0.0034	
ω (Hip) [deg]		256.2 ± 2.1	

[a]Assumed.

[b]$L_1 + L_2 + L_3 = 1$

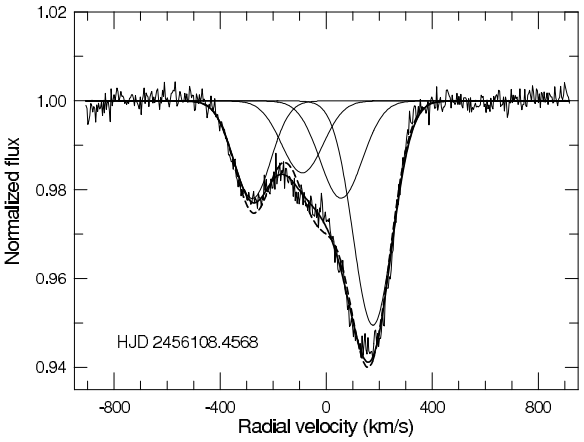

Fig. 5.— An example of a He I 4922 Å profile where the two-line fit of the third-body contribution is neessary. Dashed curve shows the best one-line fit.

Buscombe, W., & Kennedy, P.M. 1969, MNRAS, 143, 1

Campbell, W.W. 1928, Publ. Lick Obs., 16, 221

Claret, A. 2004, A&A, 424, 919

Conti, P.S., & Alschuler, W.R. 1971, ApJ, 170, 325

Conti, P.S., Leep, E.M., & Lorre, J.J. 1977, ApJ, 214, 759

Cousins, A.W.J., & Stoy, R.H. 1962, Roy. Greenwich Obs. Bull., 64, 103

Feast, M.W., Thackeray, A.D., & Wesselink, A.J. 1957, Mem. R. Astron. Soc., 68, 1

Ferrero, G., Gamen, R., Benvenuto, O., & Fernández-Lajús, E. 2013, MNRAS, 433, 1300

Hadrava, P. 2004a, Publ. Astron. Inst. Acad. Sci. Czech Rep., 89, 1

Hadrava, P. 2004b, Publ. Astron. Inst. Acad. Sci. Czech Rep., 89, 15

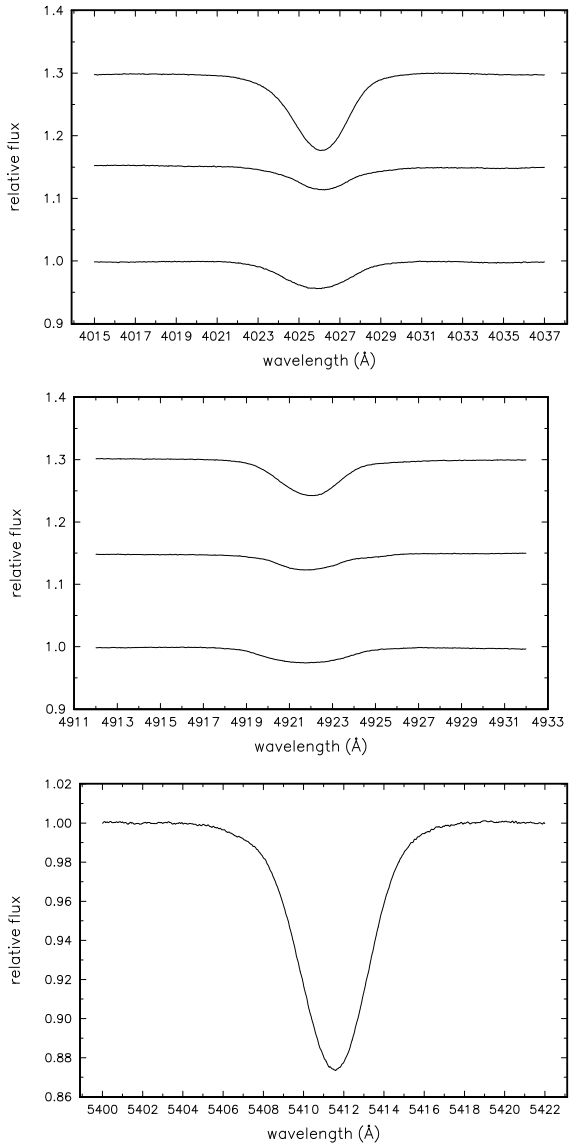

Fig. 6.— The line profiles of the primary (top profile in each panel), secondary, and tertiary as disentangled by KOREL

.

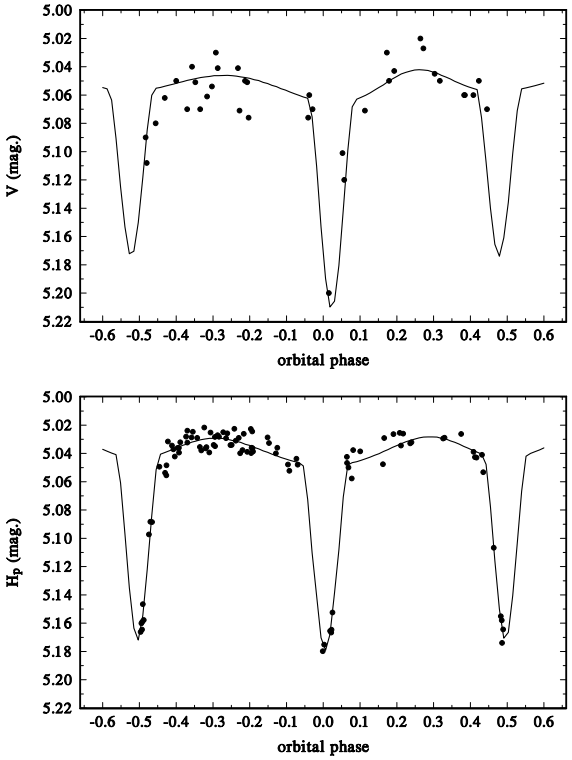

Fig. 8.— A comparison of observed light curves and PHOEBE model light curves. Upper panel: Cousins Cape V photometry. Bottom panel: Hipparcos $H_{\rm p}$ photometry.

Hill, G. 1982, Publ. DAO, 16, 67

Hiltner, W.A., Garrison, R.F., & Schild, R.E. 1969, ApJ, 157, 313

Horn, J., Kubát, J., Harmanec, P., et al. 1996, A&A, 309, 521

Kaufer, A., & Pasquini, L. 1998, SPIE, 3355, 844

Lanz, T., & Hubeny, I. 2003, ApJS, 146, 417

Le Bouquin, J.-B., Berger, J.-P., Lazareff, B., et al. 2011, A&A, 535, A67

Martins, F., Schaerer, D., & Hillier, D.J. 2005, A&A, 436, 1049

Mayer, P., Harmanec, P., Nesslinger, S., et al. 2008, A&A, 481, 183

Mayer, P., Drechsel, H., Harmanec, P., Yang, S., & Šlechta, M. 2013, A&A, 559, A22

Morrell, N.I., Barbà, R.H., Niemela, V.S., et al. 2001, MNRAS, 326, 85

Penny, L.R., Seyle, D., Gies, D.R., et al. 2001, AJ, 548, 889

Perryman, M. A. C. & ESA 1997, The HIPPARCOS and TYCHO catalogues (Publisher: Noordwijk, Netherlands: ESA Publications Division, Series: ESA SP Series 1200)

Pojmanski, G. 2002, Acta Astron., 52, 397

Poretti, E., Rainer, M., Mantegazza, L., et al. 2013, Astroph. and Space Sci. Proc., 31, 39

Prša, A., & Zwitter, T. 2005, ApJ, 628, 426

Sana, H., Rauw, G., & Gosset, E. 2001, A&A, 370, 121

Škoda, P. 1996, ASP Conf. Ser., 101, 187

Söderhjelm, S. 1984, A&A, 141, 232

Stickland, D.J., Koch, R.H., Pachoulakis, I., & Pfeiffer, R.V. 1993, Observatory, 113, 139

Thackeray, A.D., & Emerson, B. 1969, MNRAS, 142, 429

Walborn, N.R., 1972, AJ, 77, 312

This 2-column preprint was prepared with the AAS LaTeX macros v5.2.